Dynamical evolution of gravitational waves in asymptotically de Sitter spacetime

Masaru Shibata,[1] Ken-ichi Nakao,[2] Takashi Nakamura,[3] and Kei-ichi Maeda[4]
[1]*Department of Earth and Space Science, Faculty of Science, Osaka University, Toyonaka, Osaka 560, Japan*
[2]*Department of Physics, Kyoto University, Kyoto 606-01, Japan*
[3]*Yukawa Institute for Theoretical Physics, Kyoto University, Kyoto 606-01, Japan*
[4]*Department of Physics, Waseda University, Tokyo 169-50, Japan*
(Received 17 November 1993)

We perform numerical computations to investigate the dynamical evolution of axisymmetric gravitational waves in asymptotically de Sitter spacetime. The final fates of such spacetimes are classified into two types: (1) de Sitter spacetime with small perturbations, and (2) Schwarzschild–de Sitter–like spacetime with both black-hole and cosmological apparent horizons. We also find that if the mass of gravitational waves is larger than the critical value, $M_{\rm crit} \equiv (3\sqrt{\Lambda})^{-1}$, then the black hole is not formed even in the case that there exist highly nonlinear localized gravitational waves. In such a case, the Universe is initially dominated by gravitational waves rather than a cosmological constant Λ and eventually approaches a de Sitter universe. These results are consistent with the previous analysis by use of initial data.

PACS number(s): 98.80.Hw, 04.20.Jb, 04.30.Db

I. INTRODUCTION

Gravitational collapse is one of the most important issues in general relativity. In asymptotically flat spacetime, it is well known that the concentration of a large amount of inhomogeneities causes the trapped region and results in the formation of a black hole if cosmic censorship is true [1]. If the scale of the collapsing objects is much smaller than the cosmological horizon, asymptotic flatness is a good approximation. However, if the scale of the collapsing object is comparable to the cosmological horizon scale, what happens?

In the very early stage of the Universe, we have very little information about the inhomogeneities of matter and the structure of the Universe. Spacetime might be very chaotic and highly inhomogeneous. On the other hand, the present Universe is quite isotropic and homogeneous, at least after the recombination era. If the initial state of the Universe is not so isotropic and homogeneous, what makes the present Universe as it is? The inflationary scenario seems to be one of the most elegant and natural solutions for it [2]. If the de Sitter universe (an inflationary phase) is the attractor of spacetimes with a cosmological constant Λ, i.e., if the so-called cosmic no-hair conjecture [3] (CNC) is true, inflation is a quite natural and universal phenomenon in the history of the Universe. The present isotropy and homogeneity of the Universe is easily understood.

Therefore, in connection with the CNC, as well as from the point of view of mathematical simplicity, the behavior of inhomogeneities in asymptotically de Sitter spacetime [4] is an interesting subject to show the generality of inflation. From the point of view of dynamics of general relativity, it is also important to see the difference between gravitational collapse in asymptotically flat spacetime and the cosmological one.

There are analytic "black-hole" solutions in asymptotically de Sitter spacetime (the Kerr–Newman–de Sitter family [5]), which may give insight into the final state of the gravitational collapse, although it has not been shown whether or not the Kerr–Newman–de Sitter family is a unique stationary black-hole solution of the vacuum Einstein equations with a positive cosmological constant Λ. One of the remarkable properties of this family is that there is a critical value for the "gravitational mass," beyond which there is no black-hole event horizon. Hence it is expected that inhomogeneities with a gravitational mass larger than the critical mass cannot collapse into a black hole in asymptotically de Sitter spacetime.

Analysis of spherically symmetric dust collapse in a spacetime with $\Lambda > 0$ shows that the dust ball with a gravitational mass larger than a critical value cannot form a black hole. The critical value agrees with that of Schwarzschild–de Sitter spacetime, i.e., $M_{\rm crit} \equiv (3\sqrt{\Lambda})^{-1}$, where Schwarzschild–de Sitter spacetime is a spherically symmetric and charge-neutral member of the Kerr–Newman–de Sitter family [6]. This result is not so surprising since we can show by Birkhoff's theorem that a spherically symmetric vacuum spacetime with Λ is always a Schwarzschild–de Sitter spacetime. However, in the axially symmetric case, solving initial data, Nakao *et al.* have also shown that nonrotating inhomogeneities (gravitational waves [7] or Einstein-Rosen bridges [8]) with a gravitational mass larger than $M_{\rm crit}$ do not produce an apparent horizon enclosing themselves in three-space with constant-mean-curvature time slicing condition. Even though their analysis is restricted only to initial data, the results suggest that inhomogeneities with the gravitational mass larger than $M_{\rm crit}$ cannot collapse into a black hole. Furthermore, because of the coincidence of the critical value $M_{\rm crit}$, Schwarzschild–de Sitter spacetime seems to be a unique solution with asymptotically de Sitter spacetime for the static vacuum Einstein equations with Λ.

In this paper, we investigate the dynamical evolution of the axisymmetric and nonrotating gravitational waves in asymptotically de Sitter spacetime. Our motivation is to investigate the nonlinear dynamics of the gravitational waves in the cosmological scale and to confirm the above conjecture obtained by analysis of the initial data.

This paper is organized as follows. In Sec. II we express the Einstein equations in an appropriate form for the numerical simulation of the nonlinear gravitational waves in asymptotically de Sitter spacetime. In Sec. III we present the definition of black-hole and cosmological apparent horizons and the equations for those horizons. The numerical results are shown in Sec. IV. Finally, in Sec. V we summarize our results and discuss the implication to the CNC and the relation between our results and recent topics about black holes in asymptotically de Sitter spacetime [4,9,10].

In this paper, we follow Misner, Thorne, and Wheeler (MTW) [11] for the sign convention of metric and Riemann tensors, etc. The Latin indices take 1,2,3, while Greek indices take 0,1,2,3.

II. BASIC EQUATIONS

In 3+1 formalism, the line element is written as

$$ds^2=-N^2dt^2+\gamma_{ij}(dx^i-N^idt)(dx^j-N^jdt)\ , \tag{2.1}$$

where N, N^i, and γ_{ij} are the lapse function, shift vector, and intrinsic metric of the three-space, respectively [13,14]. N and N^i are purely coordinate variables and are determined by the time slicing and spatial gauge conditions. Then the 3+1 forms of the vacuum Einstein equations with Λ are written as

$$R+K^2-K_{ij}K^{ij}=2\Lambda\ , \tag{2.2}$$

$$D_iK^i_j-D_jK=0\ , \tag{2.3}$$

$$\partial_t\gamma_{ij}=-2NK_{ij}-D_iN_j-D_jN_i\ , \tag{2.4}$$

$$\partial_tK^i_j+N^lK^i_{j,l}=N^i{}_{,k}K^k_j-N^k{}_{,j}K^i_k-D^iD_jN+N(R^i_j+KK^i_j-\Lambda\delta^i_j)\ , \tag{2.5}$$

where R, R_{ij}, and D_i are the Ricci scalar, Ricci tensor, and covariant derivative within the three-space, respectively. ∂_t and $,i$ are the ordinary derivatives with respect to t and x^i.

As we discussed in the Introduction, we are interested in the effect of Λ on the dynamics of the Universe. We expect that the behavior of a solution with Λ is quite different from that without Λ. In order to see the role of Λ more clearly and further to integrate easily the above equations numerically, we adopt the appropriate dynamical variables and time slicing condition [12].

First, we adopt the conformally transformed metric $\tilde{\gamma}_{ij}$ as a dynamical variable, which is defined by

$$\gamma_{ij}=\phi^4\tilde{\gamma}_{ij}\ , \tag{2.6}$$

where ϕ is the conformal factor. It will be fixed later. As for K^i_j, we decompose it into the trace and trace-free parts as

$$K^i_j=\tfrac{1}{3}\delta^i_jK+L^i_j\ . \tag{2.7}$$

Furthermore, we introduce the conformally weighted trace-free part of the extrinsic curvature $\tilde{L}^i_j=\phi^6L^i_j$ to simplify the Einstein equations. We do not regard the trace part of the extrinsic curvature K as a dynamical variable, but we fix it to some appropriate constant value to impose the constant-mean-curvature time slicing condition. Here we fix K as

$$K=-3H\ \text{ with }\ H\equiv\left[\frac{\Lambda}{3}\right]^{1/2}\ . \tag{2.8}$$

Then the Einstein equations (2.2)–(2.5) become

$$8\phi^{-5}\tilde{D}^l\tilde{D}_l\phi-\phi^{-4}\tilde{R}+\tilde{L}^i_j\tilde{L}^j_i\phi^{-12}=0\ , \tag{2.9}$$

$$\tilde{D}_i\tilde{L}^i_j=0\ , \tag{2.10}$$

$$\partial_t\ln\tilde{\gamma}+12\partial_t\ln\phi=2(3HN-D_kN^k)\ , \tag{2.11}$$

$$\partial_t\tilde{\gamma}_{ij}-\frac{\partial_t\tilde{\gamma}}{3\tilde{\gamma}}\tilde{\gamma}_{ij}=-\phi^{-4}(2N\tilde{L}_{ij}\phi^{-6}+D_iN_j+D_jN_i-\tfrac{2}{3}h_{ij}D_kN^k)\ , \tag{2.12}$$

$$D^lD_lN=N\tilde{L}^i_j\tilde{L}^j_i\phi^{-12}\ , \tag{2.13}$$

$$\partial_t\tilde{L}^i_j+(N^l\hat{\tilde{L}}^i_j)_{,l}+\frac{1}{2\tilde{\gamma}}(\partial_t\tilde{\gamma}+N^l\tilde{h}_{,l})\tilde{L}^i_j=N^i{}_{,k}\tilde{L}^k_j-N^k_{,j}\tilde{L}^i_k-\phi^6D^iD_jN+N\phi^6R^i_j\ , \tag{2.14}$$

where $\tilde{D}_j$ and $\tilde{R}$ are the covariant derivative and the scalar curvature with respect to $\tilde{\gamma}_{ij}$, respectively, and $\tilde{\gamma}$ is the determinant of $\tilde{\gamma}_{ij}$. Note that we have used both D_l and $\tilde{D}_l$ for brevity in the description of those equations. Except for Eq. (2.11), the above equations do not contain Λ and they are the same equations as in the case of $\Lambda=0$.

Here it should be noted that, in the case of the homogeneous and isotropic universe with the conventional gauge condition ($\tilde{\gamma}=N=1$ and $N^k=0$), Eq. (2.11) with the condition (2.8) corresponds to the Freidmann equation and results in de Sitter spacetime with a scale factor $a(t)=\phi^2\propto e^{Ht}$. Hence the asymptotically de Sitter condition simply reduces to the flatness of three-space in the spatial asymptotic region ($\tilde{\gamma}\to1$, $N\to1$, and $N^k\to0$ for $r\to\infty$). The asymptotic behavior of ϕ is given by $\phi\to e^{Ht/2}$. Therefore we shall introduce a conformal factor ψ as

$$\phi=\sqrt{a(t)}\psi\ \text{ with }\ a(t)\equiv e^{Ht}\ , \tag{2.15}$$

so that $\psi\to1$ for $r\to\infty$. Further, if we see the time evolution of the right-hand side of Eq. (2.14) in the asymptotically de Sitter region, we find that it behaves as $\propto a$. Then we rewrite $\tilde{L}^j_i$ as $\tilde{L}^j_i=aA^j_i$. Those equations become

$$8\psi^{-5}\tilde{D}^l\tilde{D}_l\psi-\psi^{-4}\tilde{R}+A^i_jA^j_i\psi^{-12}a^{-2}=0\ , \tag{2.16}$$

$$\tilde{D}_iA^i_j=0\ , \tag{2.17}$$

$$\partial_t\ln\tilde{\gamma}+12\partial_t\ln\psi=2[3H(N-1)-D_kN^k]\ , \tag{2.18}$$

$$\partial_t\tilde{\gamma}_{ij}-\frac{\partial_t\tilde{\gamma}}{3\tilde{\gamma}}\tilde{\gamma}_{ij}=-2NA_i^k\tilde{\gamma}_{kj}\psi^{-6}a^{-2}$$
$$-2\tilde{\gamma}_{k(i}D_{j)}N^k+\tfrac{2}{3}\tilde{\gamma}_{ij}D_kN^k\ , \tag{2.19}$$

$$D^lD_lN=NA_j^iA_i^j\psi^{-12}a^{-4}\ , \tag{2.20}$$

$$\partial_tA_j^i+2HA_j^i+(N^lA_j^i)_{,l}+\frac{1}{2\tilde{\gamma}}(\partial_t\tilde{\gamma}+N^l\tilde{\gamma}_{,l})A_j^i$$
$$=N^i_{,k}A_j^k-N^k_{,j}A_k^i-\psi^6a^2(D^iD_jN-NR_j^i)\ . \tag{2.21}$$

As for the spatial coordinate condition, we adopt the isothermal gauge [14], in which the line element becomes

$$ds^2=-N^2dt^2+a^2\psi^4[B^{-2}\{(dr-N^rdt)^2+r^2(d\theta-N^\theta dt)^2\}$$
$$+B^2r^2\sin^2\theta\,d\varphi^2]\ . \tag{2.22}$$

By virtue of the above coordinate choice, $\partial_t\ln\tilde{\gamma}$ is equal to $-2\partial_t\ln B$ and hence Eq. (2.18) is regarded as the evolution equation for ψ while Eq. (2.19) is that for B. However, since we will determine ψ by solving the Hamiltonian constraint (2.16), we do not need Eq. (2.18).

We introduce η as $B^2\equiv1+\eta\sin^2\theta$. For the case without Λ, η is regarded as the + mode gravitational waves in the wave zone. Therefore we solve the evolution equation for η rather than for B. Further, to guarantee regularity on the symmetry axis, we use the variables

$$A_1\equiv A_r^r\ ,\quad A_2\equiv\frac{rA_r^\theta}{\sin\theta}\ ,\quad A_p\equiv\frac{A_\varphi^\varphi-A_\theta^\theta}{2\sin^2\theta}\ ,$$
$$N_1\equiv N^r/r,\quad G\equiv N^\theta/\sin\theta\ . \tag{2.23}$$

Then, choosing the $y=r^2$ and $x=\cos\theta$ as the independent variables, the basic equations finally become as follows.

(1) Evolution equation of η:

$$\partial_t\eta+2N_1\eta_{,y}-G(1-x^2)\eta_{,x}=-G_{,x}-2NA_p\psi^{-6}a^{-2}-\eta[2Gx+(G_{,x}+2NA_p\psi^{-6}a^{-2})(1-x^2)]\ . \tag{2.24}$$

(2) Evolution equations of the extrinsic curvature:

$$\frac{dA_1}{dt}=-B^2\psi^2\left[4yN_{,yy}+2N_{,y}\left\{1+2\frac{B_{,y}}{B}y-4\frac{\psi_{,y}}{\psi}y\right\}+\frac{1-x^2}{y}\left\{2\frac{\psi_{,x}}{\psi}-\frac{B_{,x}}{B}\right\}N_{,x}\right]$$
$$-NB^2\left[16\psi(\psi_{,yy}y+\psi_{,y})-16\psi_{,y}^2y+16\psi\psi_{,y}\frac{B_{,y}}{B}y+4\psi^2\left\{2\frac{B_{,y}^2}{B^2}y+\frac{B_{,y}}{B}\right\}\right.$$
$$\left.+\frac{2}{y}[\psi\psi_{,xx}(1-x^2)-2\psi\psi_{,x}x+\psi_{,x}^2(1-x^2)]-\frac{\psi^2}{yB}[B_{,xx}(1-x^2)-2B_{,x}x]\right]$$
$$+A_1\left[-3N_1+\frac{3}{2}G_{,x}(1-x^2)-3Gx+\frac{3N}{2\psi^6}a^{-2}A_1\right]-2A_2(1-x^2)(2G_{,y}y+NA_2\psi^{-6}a^{-2})\ , \tag{2.25}$$

$$\frac{dA_p}{dt}=-B^2\psi^2\left[\frac{N_{,xx}}{2y}-4N_{,y}\frac{\eta_{,y}}{B^2}y-4\frac{\psi_{,x}}{\psi y}N_{,x}\right]$$
$$-\frac{NB^2\psi^2}{2}\left[8\frac{\psi_{,y}}{\psi}\frac{\eta_{,y}}{B^2}y+4\frac{\eta_{,yy}}{B^2}y-2\frac{\eta_{,y}^2}{B^3}y(1-x^2)+6\frac{\eta_{,y}}{B^2}+\frac{1}{y}\left\{-2\frac{\psi_{,xx}}{\psi}+6\left\{\frac{\psi_{,x}}{\psi}\right\}^2(1-x^2)+\frac{B_{,xx}}{B}-2\frac{B_{,x}^2}{B^2}\right\}\right]$$
$$+A_p\left[-3N_1+\frac{3}{2}G_{,x}(1-x^2)-5Gx+\frac{3N}{2\psi^6}a^{-2}A_1\right]-A_2(2G_{,y}y+NA_2\psi^{-6}a^{-2})\ , \tag{2.26}$$

$$\frac{dA_2}{dt}=-B^2\psi^2\left[-2N_{,xy}+2N_{,y}\left\{-\frac{B_{,x}}{B}+2\frac{\psi_{,x}}{\psi}\right\}+\left\{4\frac{\psi_{,y}}{\psi}-2\frac{B_{,y}}{B}+\frac{1}{y}\right\}N_{,x}\right]$$
$$-NB^2\psi^2\left[-4\frac{\psi_{,xy}}{\psi}+12\frac{\psi_{,x}\psi_{,y}}{\psi^2}-\frac{4}{\psi B}(\psi_{,y}B_{,x}+\psi_{,x}B_{,y})-2\frac{B_{,xy}}{B}-4\frac{B_{,x}B_{,y}}{B^2}+2x\frac{\eta_{,y}}{B^2}+\frac{1}{y}\left\{\frac{2\psi_{,x}}{\psi}-\frac{B_{,x}}{B}\right\}\right]$$
$$+A_2\left[-3N_1+\frac{3}{2}G_{,x}(1-x^2)-4Gx+\frac{N}{\psi^6}a^{-2}[3A_1+A_p(1-x^2)]\right]+G_{,y}y[3A_1+A_p(1-x^2)]\ , \tag{2.27}$$

where the operator d/dt is defined by

$$\frac{dX}{dt}\equiv\partial_tX+N^iD_iX$$
$$=\partial_tX+HX+2N_1X_{,y}-G(1-x^2)X_{,x}\ . \tag{2.28}$$

(3) The equation for ψ (Hamiltonian constraint):

$$4\psi_{,yy}y+6\psi_{,y}+4\frac{B_{,y}}{B}\psi_{,y}y+\frac{1}{y}\left[\psi_{,xx}(1-x^2)-2\psi_{,x}x+\frac{B_{,x}}{B}\psi_{,x}(1-x^2)\right]$$

$$=-\frac{1}{8B^2\psi^7a^2}\left[\frac{3}{2}A_1^2+2A_2^2(1-x^2)+2A_p^2(1-x^2)^2\right]-\frac{\psi}{4B^2}\left[4B_{,y}(By)_{,y}+\frac{B_{,x}}{y}(B_{,x}(1-x^2)-2Bx)\right] . \quad (2.29)$$

(4) The equation for the shift vector (isothermal gauge condition):

$$2yN_{1,y}=Gx-G_{,x}(1-x^2)-\frac{N}{2\psi^6a^2}[3A_1+2A_p(1-x^2)] ,$$
$$N_{1,x}=2G_{,y}y+2\frac{N}{\psi^6a^2}A_2 . \quad (2.30)$$

(5) The equation for the lapse function (constant mean curvature condition):

$$4N_{,yy}y+6N_{,y}+4\frac{B_{,y}}{B}N_{,y}y+8\frac{\psi_{,y}}{\psi}N_{,y}y+\frac{1}{y}\left[N_{,xx}(1-x^2)-2N_{,x}x+\frac{B_{,x}}{B}N_{,x}(1-x^2)+2\frac{\psi_{,x}}{\psi}N_{,x}(1-x^2)\right]$$
$$=\frac{N}{B^2\psi^8a^2}\left[\frac{3}{2}A_1^2+2A_2^2(1-x^2)+2A_p^2(1-x^2)^2\right] . \quad (2.31)$$

These equations are the same as those of asymptotically flat spacetime without Λ in the isothermal gauge and the maximal time slice conditions [14] except for the viscosity term proportional to H in the differential operator d/dt and the decaying terms such as A_{ij}/a^2 in the evolution equations. Therefore we can easily generalize a numerical code for the asymptotically flat spacetime to that for the asymptotically de Sitter spacetime if we adopt the constant-mean-curvature slice condition (2.8).

Numerical methods to solve the evolution equations (2.24)–(2.27) are the same as those shown by Stark and Piran [13]. To solve the shift equation (2.30), we introduce two potential χ_1 and χ_2, and we define N_1 and G as

$$N_1=2y\chi_{1,y}+\chi_2x-(1-x^2)\chi_{2,x} ,$$
$$G=2y\chi_{2,y}+\chi_{1,x} . \quad (2.32)$$

Then the equations for χ_1 and χ_2 become

$$4y(\chi_{1,y}y)_{,y}+\chi_{1,xx}(1-x^2)-\chi_{1,x}x$$
$$=-\frac{N}{\psi^6a^2}\left[\frac{3}{2}A_1+A_p(1-x^2)\right] , \quad (2.33)$$

$$4y(\chi_{2,y}y)_{,y}+\chi_{2,xx}(1-x^2)-3\chi_{2,x}x-\chi_2=-\frac{2N}{\psi^6a^2}A_2 . \quad (2.34)$$

Hence we must solve four elliptical equations [Eqs. (2.16), (2.21), (2.33), and (2.34)] at each time step. The boundary conditions for these equations are completely the same as those for the asymptotically flat spacetime by virtue of our appropriate choice of variables. In order to solve these equations, we use the ILUCGS method [15], which is an improved version of the ICCG method [16] and can be used in the case of the asymmetric matrix.

To check the numerical accuracy, we use the momentum constraint (MC), which is now written as $D_iK^i_j=0$ rather than $\tilde{D}_iA^i_j=0$ because the accuracy should be checked in the physical frame. We define the accuracy at each grid point n in the simulation as

$$A_k=\frac{|D_iK^i_j|_k}{\sum|(\text{each term of the MC})_k|} . \quad (2.35)$$

In the numerical calculations shown below, it is found that the averaged relative error

$$\frac{1}{n}\sum_{k=1}^{n}A_k , \quad (2.36)$$

where n is a total grid number, is guaranteed within 1%.

III. APPARENT HORIZON

One of the purposes of our numerical computations is to investigate whether or not the nonlinear gravitational waves do collapse into a black hole. A black hole is characterized by the event horizon [17]. However, the event horizon can be found only when we get all the data of a spacetime, and hence it is impossible to determine the event horizon only by the finite numerical data. Instead of the event horizon, the apparent horizon is often used in numerical relativity as an approximate notion of the event horizon. The apparent horizon coincides with the outermost spacelike closed two-surface such that the expansion of the future-directed outgoing null geodesic congruence orthogonal to the two-surface vanishes. In the case of asymptotically flat spacetime, assuming cosmic censorship [1], the apparent horizon always lies inside the event horizon [17]. Shiromizu *et al.* have shown that the same is true also for asymptotically de Sitter

spacetime [4]. Therefore we may conclude that a black hole exists if we find the apparent horizon.

In contrast with asymptotically flat spacetime, there is another kind of apparent horizon called the "cosmological apparent horizon" (CAH) [7]. A CAH is defined by the closed spacelike two-surface such that the expansion of future-directed ingoing null geodesic congruence orthogonal to the two-surface vanishes and further the surface can be deformed slightly outward so that the expansion of the future-directed ingoing null geodesic congruence orthogonal to this two-surface is everywhere positive. The area of the CAH is a measure of the strength of cosmic expansion. We shall call the apparent horizon defined first in the above a "black-hole apparent horizon" (BAH) in order to distinguish it from the CAH.

The apparent horizon is found from the equation

$$(\gamma^{ij}-s^i s^j)(K_{ij}-D_i s_j)=0 , \tag{3.1}$$

where s_i is a spacelike unit vector orthogonal to the surface of the apparent horizon. When the apparent horizon is expressed by a curve of $r=w(\theta)$,

$$s_i=\frac{a\psi^2}{B}\left[1+\frac{w_{,\theta}{}^2}{r^2}\right]^{-1/2} D_i\tau , \tag{3.2}$$

where $\tau=r-w(\theta)$. Then the equation of the apparent horizon becomes

$$\begin{aligned} w_{,\theta\theta}&+\left[\frac{w_{,\theta}{}^3}{w^2}+w_{,\theta}\right]\left[4\frac{\psi_{,\theta}}{\psi}+\cot\theta\right] \\ &-w_{,\theta}{}^2\left[\frac{3}{w}+4\frac{\psi_{,r}}{\psi}\right]-2w-4w^2\frac{\psi_{,r}}{\psi} \\ &=\mp\frac{\psi^2 a}{Bw}(w^2+w_{,\theta}{}^2)^{3/2}F(K_{ij}) , \end{aligned} \tag{3.3}$$

where $-$ and $+$ signs correspond to those for the BAH and CAH, respectively. $F(K_{ij})$ is a function of K_{ij}, which is given as

$$\begin{aligned} F(K_{ij})\equiv -2H-[&w^2 A_1-2ww_{,\theta}A_2\sin\theta \\ &-\tfrac{1}{2}w_{,\theta}{}^2(A_1+2A_p\sin^2\theta)] \\ &\times(w^2+w_{,\theta}{}^2)^{-1} . \end{aligned} \tag{3.4}$$

In this paper, we assume a symmetry with respect to the equatorial plane. Then the surface of the apparent horizon must be smooth at the symmetric axis and on the equatorial plane, so that w must satisfy the boundary conditions

$$w_{,\theta}=0 \quad \text{at } \theta=0,\ \pi/2 . \tag{3.5}$$

To solve Eq. (3.3), we adopt the prescription proposed by Sasaki *et al.* [18]. The details of how to obtain both the BAH and CAH in asymptotically de Sitter space are given in Ref. [8].

IV. NUMERICAL RESULTS

A. Initial condition and measure of inhomogeneity

To set the initial conditions, we need to solve the Hamiltonian and momentum constraints. In this paper, we consider only initial conditions with $A_j^i=0$, which corresponds to time-symmetric initial data in the case of $\Lambda=0$ due to the time slicing condition (2.8). Hence the momentum constraint becomes trivial and we have only to solve the Hamiltonian constraint [Eq. (2.29)] for ψ. We set η as

$$\eta=\frac{3A}{r_0^5}\left[\frac{r_0^2}{r^2}(1-e^{-r^2/r_0^2})-e^{-r^2/r_0^2}\left[1-\frac{16r^2}{3r_0^2}+\frac{4r^4}{3r_0^4}\right]\right] , \tag{4.1}$$

where A and r_0 denote the amplitude and width of a wave packet, respectively. The amplitude A specifies the nonlinearity of the waves. To see the nonlinear effects of the waves, we change the value of the dimensionless variable A. In what follows, we set $r_0=1$; i.e., the scale length in all physical quantities is normalized by r_0. This is the reason why we have used the complicated function (4.1) as initial data for η, which is the same as that of the analytic solution of the linearized Einstein equations: As we present in the Appendix, we can solve the linearized Einstein equations with the present gauge condition. If we use the same initial data for our numerical simulation, it will be easy to compare our numerical results with the analytic ones and to check the accuracy of our numerical code.

As a measure of the inhomogeneity of spacetime, we consider the Abbott-Deser (AD) mass $M_{\rm AD}$ [19], which is the conserved "energy" associated with the timelike Killing vector in background de Sitter spacetime and coincides with the Arnowitt-Deser-Misner (ADM) mass in the limit of $\Lambda\to 0$. To calculate it easily in our formalism with the condition (2.8), we rewrite the original expression of the AD mass presented by Abbott and Deser [19] as

$$\begin{aligned} M_{\rm AD}&=\lim_{r\to\infty}\left[-\frac{a}{2\pi}\oint dS_i\sqrt{\tilde\gamma}\tilde\gamma^{ij}\partial_j\psi+\frac{Ha^3}{8\pi}\oint dS_i L_j^i x^j\right] \\ &=\lim_{r\to\infty}\left[-\frac{a}{2\pi}\int\tilde D^l\tilde D_l\psi d\tilde V+\frac{Ha}{8\pi}\oint dS_i A_j^i x^j\right] \\ &\simeq\frac{1}{4a}\int_0^1\int_0^{r_{\max}}\left[\frac{3}{2}A_1^2+\frac{2}{r^2}A_2^2(1-x^2)+2A_p^2(1-x^2)^2-\tilde R\psi^8 a^2\right]\frac{r^2 dr\,dx}{\psi^7\sqrt{1+\eta(1-x^2)}}+\frac{Ha}{2}r_{\max}^3\int_0^1 A_1|_{r=r_{\max}}dx , \end{aligned} \tag{4.2}$$

where $(x^i)=(r,0,0)$ with spherical polar coordinates. dS_i and $d\tilde{V}$ are the area element of the sphere in the background Euclid three-space and the volume element in the conformal three-space with $\tilde{\gamma}_{ij}$, respectively. To find the last equation, we have used the Hamiltonian constraint (2.91). The symbol $\simeq$ is used because $r=\infty$ is replaced with $r_{\max}$ (the numerical boundary). Here it is worthy to notice that AD mass of our initial data with $A^i_j=0$ does not depend on Λ since the second integral in each equality of Eq. (4.2) vanishes. However, in the course of time evolution, A^i_j appears and gives a large contribution to the AD mass. In Fig. 1 we show the relation between A and $M_{\rm AD}$ in our initial data. We find that $A \lesssim 1$, $M_{\rm AD} \sim (4-5)A^2$. For $A \gtrsim 1.4$, there appears a node for ψ and $M_{\rm AD}$ becomes negative, which corresponds to a closing up of the universe due to the energy of the gravitational waves, while for $A \lesssim 1.4$, $M_{\rm AD}$ is non-negative [7,20]. As for the other measure of inhomogeneity, we calculate the Weyl tensor $C_{\mu\nu\rho\sigma}$, which is decomposed into the electric and magnetic part as

$$E_{ij} \equiv C_{i\mu j\nu} n^\mu n^\nu = R_{ij} - HL_{ij} - L^l_i L_{lj} \ , \tag{4.3}$$

$$B_{ij} \equiv \tfrac{1}{2}\epsilon_i{}^{kl} C_{klj\mu} n_\mu = \epsilon_i{}^{kl} D_k L_{lj} \ , \tag{4.4}$$

where n_μ and ϵ_{ijk} are the timelike unit vector normal to three-space and the antisymmetric tensor, respectively, and we have imposed the condition (2.8) to derive the above expressions. Here it should be noted that the following relation is obtained:

$$M_{\rm AD} = -\frac{a^3}{8\pi} \lim_{r\to\infty} \oint dS_i E^i_j x^j \ . \tag{4.5}$$

Since E^i_j corresponds to the tidal force suffered by time-like observers along n_μ in the asymptotic region $r \to \infty$, the above equation shows that the AD mass may deserve the title of gravitational mass. In Fig. 2 we depict a curvature scalar $I \equiv (E^l_m E^m_l + B^l_m B^m_l)/2$ of a typical initial data. From this figure, we can see that the inhomogeneity of spacetime due to the gravitational waves is toroidal.

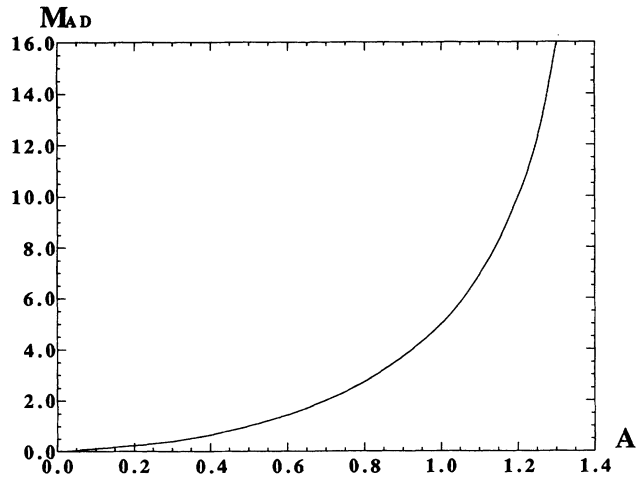

FIG. 1. Relation between the initial amplitude of the gravitational wave and its gravitational mass $M_{\rm AD}$. $M_{\rm AD}$ diverges around $A \sim 1.3$, beyond which the universe is closed and no asymptotically de Sitter region exists. It can be approximated as $M_{\rm AD} \sim (4-5) \times A^2$ for $A \leq 1$.

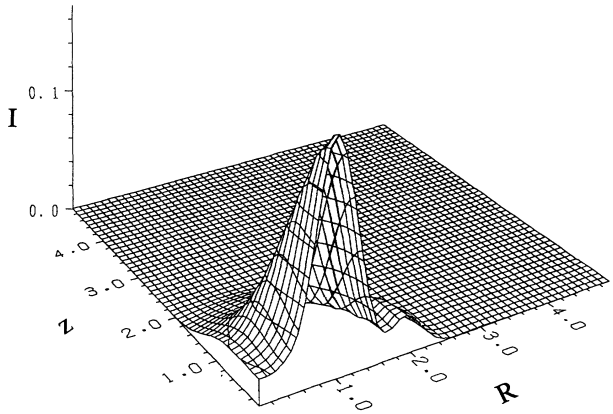

FIG. 2. Curvature scalar $I=(E^i_j E^j_i + B^i_j B^j_i)/2$ of the initial data with $A=1.0$ and $H=1.0\times10^{-2}$ is depicted. The inhomogeneity of spacetime due to the gravitational waves is toroidal.

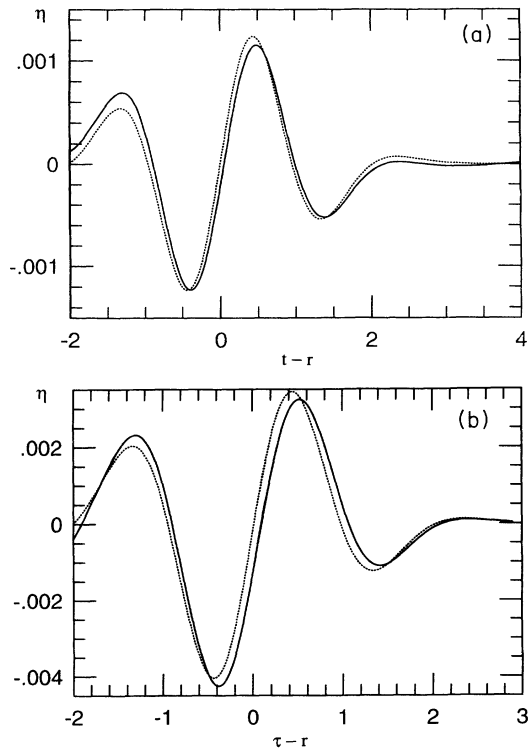

FIG. 3. Comparison of our numerical results and analytic solutions for waves with small amplitude. The radiation variable η at the numerical boundary for $\tilde{H}=0$ and at $r=3.5$ for $H=1.0\times10^{-1}$ on the equatorial plane are depicted by solid lines in the case of $A=1.0\times10^{-2}$. The analytic solutions of the linearized Einstein equations are depicted by dashed lines with same initial data. (a) is the case without Λ, while (b) is the case with $H=1.0\times10^{-1}$. The numerical results agree with the analytic solutions quite well.

B. Comparison with the analytic solutions of linear gravitational waves

If the gravitational waves are approximated as linear perturbations, i.e., $A \ll 1$, the analytic solution of the evolution equation in the isothermal gauge is obtained (see the Appendix). Hence we can check our code and further can see the nonlinearity by comparing a numerical solution with the linear solution. In Fig. 3(a) a solid line shows our numerical results of η at the numerical boundary on the equatorial plane with $A=10^{-2}$ and with $\Lambda=0$ as a function. On the other hand, in Fig. 3(b), a solid line shows the same at $r=3.5$ with $H=1.0\times10^{-1}$ on the equatorial plane by a solid line. The reason why the value is estimated at $r=3.5$ in the case of $H=1.0\times10^{-1}$ is that the gravitational waves are dumped by cosmic expansion due to Λ before those reach the numerical boundary. The corresponding pictures of the analytic solutions of the linearized Einstein equations are shown by a dashed line. These calculations are performed with the number of the numerical grids 100×16. These figures show that low amplitude gravitational waves obtained numerically agree with the analytic linear waves quite well.

C. Time evolution without a Λ term

For comparison with the asymptotically de Sitter case, we first calculated the evolution of the gravitational waves in asymptotically flat spacetime, i.e., the case of $\Lambda=0$. In our numerical calculations, we mainly investigated whether or not a black hole is formed. To investigate it, we shall look for the BAH because if it exists, the event horizon also does. However, even in the case that the BAH is not formed, the event horizon might be formed. Hence we also watch the behavior of the lapse function N at the origin and we regard that the event horizon is not formed if N at the origin bounces at some minimum value and then approaches unity. In all the present calculations, if N becomes small at the origin, a BAH is always formed.

The results obtained are essentially the same as those calculated by Miyama [21]: For small $A \lesssim 0.7$ (case Ia), all parts of the wave disperse. However, for larger A, $0.7 \lesssim A \lesssim 1$ (case IIa), although the outer part of the wave disperses, the inner part of it collapses and a BAH is formed in the course of time evolution. For larger $A \gtrsim 1$ (case IIb), the BAH surrounding the central part of the waves already exists in initial stage.

D. Time evolution with a Λ term

We have performed numerical computations for $A=0.01$, 0.3, 0.8, 1.0, and 1.3 and various values of Λ. Then we look for the formation of the BAH and CAH. Here it should be noted that the CAH depends on the location of an "observer." However, our interest is the effect of the gravitational waves on cosmic expansion and hence we focus on the CAH enclosing the center in our simulation.

In Fig. 4 we show the summary of our results. According to it, the time evolution of gravitational waves is

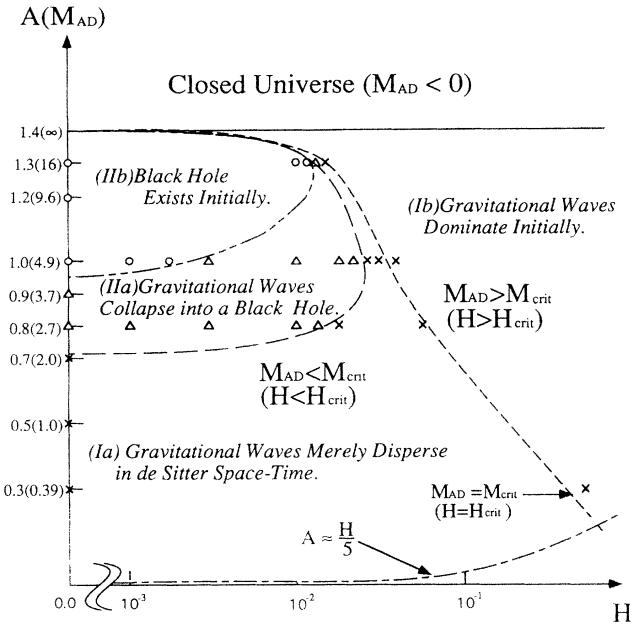

FIG. 4. Summary of the numerical results for the cases with $\Lambda>0$. The circles denote that the BAH always exists from initial data, while the triangles denote that the BAH appears in the course of time evolution. The cross corresponds to the case that a BAH does not appear. We can classify our results into four cases (Ia), (Ib), (IIa), and (IIb) (see text).

classified into the following four types.

(Ia) The BAH does not appear, but the CAH exists throughout time evolution and the area of the CAH is almost the same as that of de Sitter spacetime. The parameters of this case are given by

$$A=0.01\ (M_{\rm AD}=0.03)\ \text{for all } H\ ,$$

$$A=0.3\ (M_{\rm AD}=0.39)\ \text{for } 0\le H\lesssim H_{\rm crit}=4.9\times10^{-1}\ ,$$

$$A=0.8\ (M_{\rm AD}=2.7)$$

$$\text{for } 2.0\times10^{-2}\lesssim H\lesssim H_{\rm crit}=7.12\times10^{-2}\ ,$$

$$A=1.0\ (M_{\rm AD}=4.9)$$

$$\text{for } 3.0\times10^{-2}\lesssim H\lesssim H_{\rm crit}=3.93\times10^{-2}\ ,$$

where $H_{\rm crit}\equiv(\sqrt{27}M_{\rm AD})^{-1}$ is the critical value of Schwarzschild–de Sitter spacetime with the same gravitational mass. Note that there is no condition such as $H\lesssim H_{\rm crit}$ for $A=0.01$. We will discuss this point later.

(Ib) Only the CAH exists throughout time evolution, but in contrast with case (Ia), the area of the CAH is rather small compared with that of de Sitter spacetime, $4\pi H^{-2}$. The parameters for this case are given by

$$A=0.3\ \text{ for } H\gtrsim H_{\rm crit}=4.9\times10^{-1}\ ,$$

$$A=0.8\ \text{ for } H\gtrsim H_{\rm crit}=7.1\times10^{-2}\ ,$$

$$A=1.0\ \text{ for } H\gtrsim H_{\rm crit}=3.9\times10^{-2}\ ,$$

$$A=1.3\ \text{ for } H\gtrsim H_{\rm crit}=1.3\times10^{-2}\ .$$

This region is clearly characterized by $H > H_{\rm crit}$. These gravitational waves have a gravitational mass larger than the critical value $M_{\rm crit} \equiv (\sqrt{27}H)^{-1}$. The time variation of the area of the CAH normalized by the de Sitter value $S_{\rm deS} \equiv 4\pi H^{-2}$ is given in Fig. 5. From this figure we can see that the area of the CAH increases monotonically in the course of time evolution. This tendency is clearly different from de Sitter spacetime in which the area of the CAH is constant in time. Hence the region within the CAH can be regarded as the gravitational-wave-dominant universe. In other words, the cosmic expansion of this region is caused by the energy of the gravitational waves themselves rather than Λ, and hence the gravitational collapse and formation of a black hole are prevented even if there are highly nonlinear gravitational waves.

The fate of this type of spacetimes is expected to be again a de Sitter universe. In fact, in the case of $A = 0.3$, we have confirmed that the area of the CAH approaches asymptotically to that of de Sitter spacetime. We expect the same also in the case of $A = 0.8$, but we could not confirm it because the CAH shrinks in our coordinates and necessary grid points to resolve the CAH cannot be kept until the area reaches the value of de Sitter space.

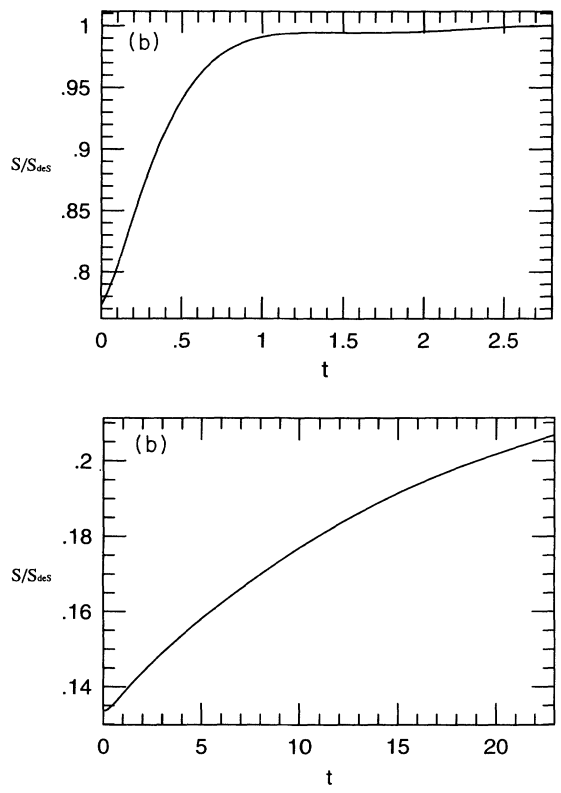

FIG. 5. Time variation of the area of the CAH normalized by the de Sitter value $S_{\rm deS} \equiv 4\pi H^{-2}$ is depicted. (a) is for the case of $A = 0.3$ and $H = 7.0 \times 10^{-1} > H_{\rm crit}$, while (b) corresponds to the case of $A = 1.0$ and $H = 4.0 \times 10^{-2} > H_{\rm crit}$. In both cases, the area of the CAH monotonically increases. This means that the cosmic expansion within this CAH is caused by the energy of the gravitational waves rather than Λ. In case (a), we can see that it approaches unity around $t \sim 1$ ($\sim 0.7H^{-1}$). Hence the fate of universe is de Sitter type.

We can summarize the above numerical results such that if $H \gtrsim H_{\rm crit}$ the energy of gravitational waves contributes to the cosmic expansion [case (Ib)], while the gravitational waves behave like as the linear perturbations which do not affect the background cosmic expansion, if $H \ll H_{\rm crit}$ [case (Ia)]. The reason why it is so is as follows: $H > H_{\rm crit}$ means that the gravitational mass of the waves $M_{\rm AD} \equiv (\sqrt{27}H_{\rm crit})^{-1}$ is larger than $M_{\rm crit} \equiv (\sqrt{27}H)^{-1}$. Then the electric part of the Weyl tensor which comes from the gravitational waves is estimated roughly as $|E^i_j| \gtrsim M_{\rm AD}|H^{-3} \gtrsim H^2$ near the CAH, which is comparable with the strength of a four-dimensional Ricci tensor ${}^{(4)}R^{\mu}_{\nu} = 3H^2\delta^{\mu}_{\nu}$. This means that even if A is small, the back reaction of the gravitational waves to background spacetime cannot be negligible near and within the CAH. This is what happens for $A = 0.3$.

This explanation is, however, valid only for the case of $r_0 < H^{-1}$. If the width of wave packet ($r_0 = 1$) is larger than the cosmological horizon scale (H^{-1}), $M_{\rm AD}$ should be replaced with $\tilde{M}_{\rm AD} \equiv (r_0 H)^{-3} M_{\rm AD}$, which naively denotes the mass of the gravitational waves within the CAH. Hence the condition for the gravitational-wave-dominated universe is now $\tilde{M}_{\rm AD} > M_{\rm crit}$. This condition with the formula $M_{\rm AD} \sim 5A^2$ (for $A < 1$) is reduced to

$$H \lesssim \sqrt{5\sqrt{27}}A \sim 5A \ . \tag{4.6}$$

Since $H_{\rm crit} = 1$ when $A \sim 0.2$ ($M_{\rm AD} \sim 0.2$), there is a range of the gravitational-wave-dominated universe if $A > 0.2$. The range can be approximated as $H_{\rm crit} \sim 1/(25A^2) \lesssim H \lesssim 5A$ for $0.2 < A < 1$. The mass formula between $1 < A < 1.4$ is modified, and $M_{\rm AD} \to +\infty$ in the limit of $A \to 1.4$. Hence the expansion may be governed by the gravitational wave energy for wider range of H than the above one.[1]

On the other hand, for the case of $A < 0.2$, the above range vanishes. That is, the mass of the gravitational waves is always so small that the back reaction of the gravitational waves on background spacetime can be always negligible for all H. This is what happens for $A = 0.01$ in case (Ia).

(IIa) The BAH does not exist at first, but later it is formed. The CAH exists throughout time evolution. The parameters of this case are given by

$$A = 0.8 \quad \text{for } 0 \le H \lesssim 2.0 \times 10^{-2} \ ,$$

$$A = 1.0 \quad \text{for } 3.0 \times 10^{-3} \lesssim H \lesssim 3.0 \times 10^{-2} \ ,$$

$$A = 1.3 \quad \text{for } H \simeq 1.3 \times 10^{-2} \ .$$

The areas of both the BAH and CAH almost coincide with those of Schwarzschild–de Sitter spacetime. In Fig. 6 we depict the time variation of the areas of the BAH

[1]We have to note that we could not confirm those expectations numerically, because, in the case of $H > 1$, we cannot keep sufficient grid points to resolve the CAH due to its smallness and for gravitational waves due to the rapid cosmic expansion.

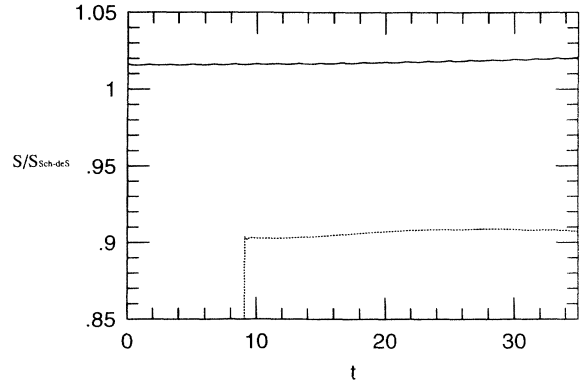

FIG. 6. Time variations of the areas of the BAH and CAH are depicted in the case of $A=1.0$ and $H=2.0\times10^{-2}<H_{\rm crit}$, which is normalized by that of Schwarzschild–de Sitter spacetime $S_{\rm Sch-deS}$ with same gravitational mass. The solid line corresponds to the CAH, while the dashed line is for the BAH. As can be seen from this figure, the BAH is formed at $t\simeq9.0$ $(\sim0.18H^{-1})$.

and CAH in the case of $A=1.0$ and $H=2.0\times10^{-2}$. The areas are normalized by those of Schwarzschild–de Sitter spacetime, $S_{\rm Sch\text{-}deS}$, with same H and same gravitational mass $M_{\rm AD}$, which was calculated at each time step by Eq. (4.2). It seems that the areas of both the BAH and CAH are almost constant.

Here we should comment on the mass conservation. Although $M_{\rm AD}$ must be constant in the course of time evolution, $M_{\rm AD}$ in our calculation slightly increases with time as a result of the truncation error. However, its relative increment to its initial value is less than a few presents at the end of our simulations. Hence these calculations have kept sufficient accuracy for our purpose.

(IIb) Both the BAH and CAH always exist from the initial stage. The parameters for this case are given by

$$A=1.0 \quad \text{for } 0\le H\lesssim 3.0\times10^{-3},$$

$$A=1.3 \quad \text{for } 0\le H\lesssim 1.2\times10^{-2}.$$

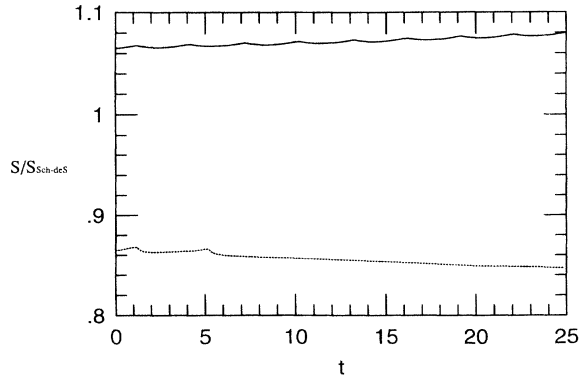

FIG. 7. Same as Fig. 6, but for $A=1.3$ and $H=1.2\times10^{-2}$. The areas of both the BAH and CAH are almost constant with respect to time.

The areas of both the BAH and CAH almost coincide with those of Schwarzschild–de Sitter spacetime (see Fig. 7).

As for the "final" states of spacetime, we can conclude that there are two types.

(I) [(a) and (b)]: de Sitter–like spacetime with small perturbations. No BAH appears. The spacetime of case (Ib) is initially a gravitational-wave-dominant universe.

(II) [(a) and (b)]: Schwarzschild–de Sitter–like spacetime with both the BAH and CAH. The spacetime of case (IIa) has no BAH initially.

We cannot make sure that the above final states are spherically symmetric because of the insufficient numerical accuracy. However, these results suggest that, in the case without rotation, the final fate of asymptotically de Sitter spacetime is some kind of Schwarzschild–de Sitter spacetime just as in the case of an asymptotically flat spacetime, in which a final state is always Schwarzschild spacetime.

V. SUMMARY AND DISCUSSIONS

In this paper, we present the concrete formalism to perform the fully relativistic numerical simulation for the gravitational waves in asymptotically de Sitter spacetime. The basic equations are the same as those of asymptotically flat spacetime with the maximal time slicing condition, except for "viscosity" and decaying terms in the dynamical equations by the background expansion. Hence we can use a numerical code for asymptotically flat spacetime to investigate asymptotically de Sitter spacetime almost as it is. Then we performed a fully relativistic numerical simulation for axisymmetric and nonrotating gravitational waves both without Λ (the asymptotically flat case) and with $\Lambda>0$ (the asymptotic de Sitter case).

The results have confirmed the conjecture obtained by the analysis of the linearized gravitational waves and the initial data of nonlinear gravitational waves. When the initial amplitude of the gravitational waves is sufficiently small, i.e., $A\lesssim0.7$ $(M_{\rm AD}\lesssim2.0)$, the gravitational waves merely disperse whether or not Λ exists. However, in the case of $\Lambda>0$, even if the gravitational waves will finally disperse, there is a qualitative change of the behavior of the gravitational waves in accordance with the value of Λ or of the gravitational mass $M_{\rm AD}$. If $H\lesssim H_{\rm crit}\equiv(\sqrt{27}M_{\rm AD})^{-1}$, i.e., $M_{\rm AD}\lesssim M_{\rm crit}\equiv(\sqrt{27}H)^{-1}$, the gravitational waves do not affect the background cosmic expansion due to Λ and therefore the behavior of those is essentially the same as the linear gravitational waves. On the other hand, when $H\gtrsim H_{\rm crit}$, i.e., $M_{\rm AD}>M_{\rm crit}$, the CAH becomes rather small initially compared with that of de Sitter spacetime and further the area of the CAH monotonically increases with time. This behavior of the area of the CAH reveals that the central region of the gravitational waves is a gravitational-wave-dominant universe. In other words, the cosmic expansion law of this region is governed by the energy of the "nonlinear" gravitational waves rather than Λ if $M_{\rm AD}>M_{\rm crit}$. This does never happen if the amplitude of the wave A is smaller than 0.2. The gravitational waves can always be regarded as linear perturbations, because the cosmic ex-

pansion is governed by Λ.

For the case of $A \gtrsim 0.8$, if $\Lambda=0$, there appears the BAH in the course of time evolution or it has already existed in the initial data. In the case of $\Lambda>0$, the BAH can also be formed if Λ is sufficiently small. However, it is a remarkable fact that when H is larger than $H_{\rm crit}$, the BAH cannot be formed. In other words, when the gravitational mass $M_{\rm AD}$ was larger than $M_{\rm crit}$, the gravitational waves do not collapse into a black hole. This result confirms the conjecture from the analysis of the initial data of nonlinear gravitational waves; i.e., the inhomogeneities with the gravitational mass larger than $M_{\rm crit}$ do not collapse into a black hole.

Recently, Shiromizu *et al.* [4] and Hayward, Shiromizu, and Nakao [9] have shown that there is an upper bound for the area of the event horizon in asymptotically flat de Sitter spacetime. This bound coincides with the maximal value of the black-hole event horizon in Schwarzschild–de Sitter spacetime, which is given by $S_{\rm max}\equiv(4\pi/3)^2H^{-2}$. Since, as in asymptotically flat spacetime, the area of the event horizon does not decrease in time also in the case of asymptotically de Sitter spacetime, black holes cannot collide each other to be a single black hole if the total area of those event horizons is larger than $S_{\rm max}$. If those black holes coalesce each other into one collapsed object, a naked singularity may appear [10]. This conclusion is consistent with our results in the sense that there does not occur a large black-hole formation in asymptotically de Sitter spacetime. However, as already mentioned in Sec. I, we have not yet proved the answer to the question of whether or not Kerr-Newman–de Sitter spacetime is unique. Hence the relation between the area of the event horizon and the gravitational mass $M_{\rm AD}$ is a nontrivial problem. However, our results obtained by the numerical simulations of nonrotating and axisymmetric gravitational waves show that the critical value for the gravitational mass $M_{\rm AD}$ or for $H=\sqrt{\Lambda/3}$ almost coincides with that of Schwarzschild–de Sitter spacetime and hence suggests the uniqueness of Schwarzschild–de Sitter spacetime.

Our results give also insight into the CNC and into an inflationary universe scenario in inhomogeneous cosmology. Black holes larger than the critical mass cannot be formed in the inflationary stage. Hence, if no naked singularity is formed, only small black holes [with mass $M\leq 10^2$ g in the grand unified theory (GUT) scale inflation] are produced through gravitational collapse of inhomogeneities and those may evaporate away through Hawking radiation or may be diluted away by exponential expansion of the Universe. As for the formation of a naked singularity, we should mention that we have never found any indication of a naked singularity in the present simulation, although the distribution of gravitational waves is fixed. In the plane-symmetric case, we have also found that no singularity appears even in highly inhomogeneous spacetimes [22]. Although the appearance of a naked singularity in a spacetime with Λ is discussed in Ref. [10], we have to study further the possibility of a naked singularity, including its generality, and to investigate its effects on the inflationary scenario, if naked singularities are formed.

ACKNOWLEDGMENTS

We would like to thank M. Sasaki and T. Shiromizu for useful discussions. This work was supported partially by a Grant-in-Aid for Scientific Research Fund of the Ministry of Education, Science and Culture (Nos. 04234104, 04640312, and 0521801), and by The Sumitomo Foundation.

APPENDIX: ANALYTIC SOLUTIONS OF THE LINEARIZED EINSTEIN EQUATIONS IN THE ISOTHERMAL GAUGE

1. Case for $\Lambda=0$

We present here the Teukolsky waves [23] in the isothermal gauge for $\Lambda=0$. The Teukolsky wave is defined in the Eulerian gauge ($N=1$, $N^i=0$), which agrees with the maximal time slicing condition in this linearized theory, and the metric of three-space is expressed as

$$\gamma_{ij}=f_{ij}+h_{ij}\ , \tag{A1}$$

where f_{ij} is the metric of flat space. In the nonrotating and axially symmetric case, h_{ij} is written as

$$h_{ij}=\begin{bmatrix} A_l^{(h)}P_l & B_l^{(h)}P_{l,\theta} & 0 \\ * & K_l^{(h)}P_l+F_l^{(h)}W_l & 0 \\ * & * & (K_l^{(h)}P_l-F_l^{(h)}W_l)\sin^2\theta \end{bmatrix}, \tag{A2}$$

where P_l is the Legendre polynomial, $W_l=P_{l,xx}(1-x^2)$ with $x=\cos\theta$, and $A_l^{(h)},B_l^{(h)},K_l^{(h)},F_l^{(h)}$ are functions of (t,r). Because h_{ij} is a transverse-traceless tensor, those four functions satisfy the relations

$$A_{l,r}^{(h)}+\frac{2}{r}A_l^{(h)}-\frac{l(l+1)}{r^2}B_l^{(h)}-\frac{2}{r^3}K_l^{(h)}=0\ , \tag{A3}$$

$$B_{l,r}^{(h)}+\frac{2}{r}B_l^{(h)}-\frac{l(l+1)-2}{r^2}F_l^{(h)}+\frac{1}{r^2}K_l^{(h)}=0\ , \tag{A4}$$

and

$$A_l^{(h)}+\frac{2}{r^2}K_l^{(h)}=0\ . \tag{A5}$$

Those three are regarded as the constraint equations because no time derivative appears. Hence there is only one degree of dynamical freedom, i.e., $A_l^{(h)}$, which satisfies

$$\frac{\partial^2 A_l^{(h)}}{\partial t^2}=\frac{\partial^2 A_l^{(h)}}{\partial r^2}+\frac{6}{r}\frac{\partial A_l^{(h)}}{\partial r}+\frac{6-l(l+1)}{r^2}A_l^{(h)}\ . \tag{A6}$$

In the case of $l=2$, the solutions are written as

$$A^{(h)}=-2\frac{K^{(h)}}{r^2}=\left[\frac{1}{r}\frac{\partial}{\partial r}\right]^2\frac{f^{(h)}(t+r)-f^{(h)}(t-r)}{r}\ , \tag{A7}$$

$$B^{(h)}=\frac{1}{6r}\frac{\partial}{\partial r}r^3A^{(h)}\ , \tag{A8}$$

and

$$F^{(h)}=\frac{1}{4}\left[-\frac{r^2}{2}+\frac{1}{6}\frac{\partial}{\partial r}r\frac{\partial}{\partial r}r^3\right]A^{(h)} . \tag{A9}$$

Here we have omitted the subscript l for brevity. Then we transform the above solution to that for the isothermal gauge. Under the gauge transformation $x^i_{\rm it}=x^i-\xi^i$, the Teukolsky wave solution $h^{\rm TW}_{ij}$ is transformed to

$$h^{\rm it}_{ij}=h^{\rm TW}_{ij}+\nabla_i\xi_j+\nabla_j\xi_i , \tag{A10}$$

where it and TW denote, respectively, the wave for the isothermal gauge and the Teukolsky wave. Under the isothermal gauge condition, the components of ξ_i satisfy

$$r^3(\xi_r/r)_{,r}-\xi_{\theta,\theta}=\tfrac{1}{2}(h^{\rm TW}_{\theta\theta}-r^2h^{\rm TW}_{rr}) \tag{A11}$$

and

$$r^2(\xi_\theta/r^2)_{,r}+\xi_{r,\theta}=-h^{\rm TW}_{r\theta} . \tag{A12}$$

The radiation variable η is written as

$$\eta=G_{,x}-\frac{3F^{(h)}}{r^2} , \tag{A13}$$

where $G=\xi^\theta/\sin\theta$, which satisfies

$$r[G_{,r}r]_{,r}+[(1-x^2)G_{,x}-Gx]_{,x}=3rx\left[\frac{B^{(h)}}{r}\right]_{,r}-\frac{3}{2}x\left[A^{(h)}-\frac{K^{(h)}}{r^2}\right]-3\frac{F^{(h)}}{r^2}x . \tag{A14}$$

Hereafter, we fix the function $f^{(h)}$ as $f^{(h)}(y)=Aye^{-y^2}$, where A is an arbitrary constant. In this case the initial condition ($t=0$) is written as

$$\begin{aligned}A^{(h)}&=-\frac{2}{r^2}K^{(h)}=\frac{8A}{r_0^5}e^{-r^2/r_0^2},\\ B^{(h)}&=\frac{4A}{r_0^4}\left[\frac{r}{r_0}\right]\left[1-\frac{2r^2}{3r_0^2}\right]e^{-r^2/r_0^2},\\ F^{(h)}&=\frac{2A}{r_0^3}\left[\frac{r}{r_0}\right]^2\left[1-\frac{8r^2}{3r_0^2}+\frac{2r^4}{3r_0^4}\right]e^{-r^2/r_0^2},\end{aligned} \tag{A15}$$

and then we obtain the solution of Eq. (A14) analytically as

$$G=\frac{3A}{r_0^5}x\left[e^{-r^2/r_0^2}+(1-e^{-r^2/r_0^2})\left[\frac{r_0}{r}\right]^2\right] , \tag{A16}$$

by which we find η of Eq. (4.1) from Eq. (A13).

In Fig. 3(a) we compare the numerical result and the analytic solution of η at the outer numerical boundary in the equatorial plane in the case that $A=0.01$.

2. Case for $\Lambda>0$

In the case with $\Lambda>0$, we can also find the analytic solution of linearized gravitational waves [12]. First, we express the metric of three-space as

$$\gamma_{ij}=a^2(t)(f_{ij}+h_{ij}) . \tag{A17}$$

Following Ref. [12], we define the variable as

$$k_{ij}=-(2H\tau)^{-1}\partial_\tau h_{ij} , \tag{A18}$$

where $\tau=-H^{-1}e^{-Ht}$ is the conformal time of background de Sitter spacetime and $k^j_j=0$ by imposing the condition (2.8). Then we can see that k_{ij} satisfies the transverse condition due to the momentum constraint (2.3) and the wave equation:

$$\tilde D_j k^j_i=0 , \tag{A19}$$

$$\partial^2_\tau k_{ij}-\tilde D^k\tilde D_k k_{ij}=0 , \tag{A20}$$

where $\tilde D_k$ is now the covariant derivative with respect to the flat metric f_{ij}. Hence we can obtain the solution for k_{ij} by the same prescription as that to obtain h_{ij} in the case of $\Lambda=0$. We write k_{ij} as

$$k_{ij}=\begin{pmatrix}A^{(k)}_lP_l & B^{(k)}_lP_{l,\theta} & 0\\ * & K^{(k)}_lP_l+F^{(k)}_lW_l & 0\\ * & * & (K^{(k)}_lP_l-F^{(k)}_lW_l)\sin^2\theta\end{pmatrix} . \tag{A21}$$

Then, in the case of $l=2$, the solutions are written as (we omit the subscript l for brevity)

$$A^{(k)}=-2\frac{K^{(k)}}{r^2}=\left[\frac{1}{r}\frac{\partial}{\partial r}\right]^2\frac{f^{(k)}(\hat\tau+r)-f^{(k)}(\hat\tau-r)}{r} , \tag{A22}$$

$$B^{(k)}=\frac{1}{6r}\frac{\partial}{\partial r}r^3A^{(k)} , \tag{A23}$$

and

$$F^{(k)}=\frac{1}{4}\left[-\frac{r^2}{2}+\frac{1}{6}\frac{\partial}{\partial r}r\frac{\partial}{\partial r}r^3\right]A^{(k)} , \tag{A24}$$

where $\hat\tau=\tau-\tau_0$ and τ is the conformal time which labels the initial three-space. Then, from Eq. (A18), we obtain the coefficient for the metric perturbation h_{ij}, i.e., $A^{(h)}_l,B^{(h)}_l,K^{(h)}_l,F^{(h)}_l$, as

$$A^{(h)}=-2\frac{K^{(h)}}{r^2}=\left[\frac{1}{r}\frac{\partial}{\partial r}\right]^2\frac{g(\hat\tau+r,\tau)-g(\hat\tau-r,\tau)}{r} , \tag{A25}$$

$$B^{(h)}=\frac{1}{6r}\frac{\partial}{\partial r}r^3A^{(h)} , \tag{A26}$$

and

$$F^{(h)}=\frac{1}{4}\left[-\frac{r^2}{2}+\frac{1}{6}\frac{\partial}{\partial r}r\frac{\partial}{\partial r}r^3\right]A^{(h)} , \tag{A27}$$

where

$$\begin{aligned}g(\hat\tau\pm r,\tau)&\equiv-2H\int_{-\infty}^{\tau}\tau' f^{(k)}(\tau'-\tau_0\pm r)d\tau'\\ &=-2H\left[\int_{-\infty}^{\hat\tau\pm r}[y-(\hat\tau\pm r)]f^{(k)}(y)dy+\tau\int_{-\infty}^{\hat\tau\pm r}f^{(k)}(y)dy\right] .\end{aligned} \tag{A28}$$

It should be noted that resultant h_{ij} becomes a transverse-traceless tensor.

Here we set the arbitrary function $f^{(k)}$ as

$$f^{(k)}(y)=-\frac{A}{2H\tau_0}\frac{d}{dy}ye^{-y^2}, \tag{A29}$$

so that $g(y,\tau)$ becomes

$$g(y,\tau)=A\left[\frac{1}{2\tau_0}+\frac{\tau}{\tau_0}y\right]e^{-y^2}. \tag{A30}$$

By virtue of the above choice (A29), $k_{ij}=0$ and h_{ij} agrees with Eq. (A14) at $\tau=\tau_0$, and therefore the initial data of G and η are also given analytically by Eqs. (A16) and (4.1).

In Fig. 3(b) we compare the numerical result and the analytic solution of η at $r=3.5r_0$ in the equatorial plane in the case that $A=0.01$ and $H=1.0\times10^{-1}$.

[1] R. Penrose, Riv. Nuovo Cimento **1** (Numero Special), 252 (1969).

[2] A. H. Guth, Phys. Rev. D **23**, 347 (1981); K. Sato, Mon. Not. R. Astron. Soc. **195**, 467 (1981); A. Albrecht and P. J. Steinhardt, Phys. Rev. Lett. **48**, 1220 (1982); A. D. Linde, Phys. Lett. **108B**, 389 (1982).

[3] G. W. Gibbons and S. W. Hawking, Phys. Rev. D **15**, 2738 (1977); S. W. Hawking and I. G. Moss, Phys. Lett. **110B**, 35 (1982); as for a review, see also, e.g., K. Maeda, in *Fifth Marcel Grossmann Meeting*, Proceedings, Perth, Australia, 1988, edited by D. G. Blair and M. J. Buckingham (World Scientific, Singapore, 1989), p. 145.

[4] T. Shiromizu, K. Nakao, H. Kodama, and K. Maeda, Phys. Rev. D **47**, R3099 (1993).

[5] B. Carter, Commun. Math. Phys. **17**, 1067 (1970); B. Carter, in *Black Holes*, edited by C. DeWitt and B. S. DeWitt (Gordon and Breach, New York, 1972); Gibbons and Hawking [3].

[6] K. Nakao, Gen. Relativ. Gravit. **24**, 1069 (1992).

[7] K. Nakao, K. Maeda, T. Nakamura, and K. Oohara, Phys. Rev. D **47**, 3194 (1993).

[8] K. Nakao, K. Yamamoto, and K. Maeda, Phys. Rev. D **47**, 3203 (1993).

[9] S. Hayward, T. Shiromizu, and K. Nakao, Phys. Rev. D **49**, 5080 (1994).

[10] D. Brill, G. Horowitz, D. Kastor, and J. Traschen, Phys. Rev. D **49**, 840 (1994).

[11] C. W. Misner, K. S. Thorne, and J. A. Wheeler, *Gravitation* (Freeman, San Francisco, 1973).

[12] K. Nakao, T. Nakamura, K. Oohara, and K. Maeda, Phys. Rev. D **43**, 1788 (1991).

[13] R. F. Stark and T. Piran, Comput. Phys. Rep. **5**, 221 (1987): In the present paper, we adopt the definition of the shift vector N^i in this reference and Ref. [14]. It should be noted that this definition of N^i is that of MTW [11] with the opposite sign.

[14] J. M. Bardeen and T. Piran, Phys. Rep. **96**, 203 (1983).

[15] I. Gustafsson, BIT **18**, 142 (1978).

[16] K. Oohara and T. Nakamura, Prog. Theor. Phys. **81**, 360 (1989).

[17] R. M. Wald, *General Relativity* (University of Chicago Press, Chicago, 1984).

[18] M. Sasaki, K. Maeda, S. Miyama, and T. Nakamura, Prog. Theor. Phys. **63**, 1051 (1980).

[19] L. Abbott and S. Deser, Nucl. Phys. **B195**, 76 (1982).

[20] D. Brill, Ann. Phys. (N.Y.) **7**, 466 (1959).

[21] S. M. Miyama, Prog. Theor. Phys. **65**, 894 (1981).

[22] H. Shinkai and K. Maeda, Phys. Rev. D **48**, 3910 (1993).

[23] S. A. Teukolsky, Phys. Rev. D **26**, 754 (1982).